Neuron
Article

Insulinoma-Associated 1 Has a Panneurogenic Role and Promotes the Generation and Expansion of Basal Progenitors in the Developing Mouse Neocortex

Lilla M. Farkas,[1] Christiane Haffner,[1] Thomas Giger,[2] Philipp Khaitovich,[2] Katja Nowick,[2,4] Carmen Birchmeier,[3] Svante Pääbo,[2] and Wieland B. Huttner[1,*]
[1]Max Planck Institute of Molecular Cell Biology and Genetics, Pfotenhauerstrasse 108, D-01307 Dresden, Germany
[2]Max Planck Institute of Evolutionary Anthropology, Deutscher Platz 6, D-04103 Leipzig, Germany
[3]Max Delbrück Center for Molecular Medicine, Robert-Rössle-Strasse 10, D-13125 Berlin, Germany
[4]Present address: Genome Biology Group, Lawrence Livermore National Laboratory, 7000 East Avenue, Livermore, CA 94550, USA
*Correspondence: huttner@mpi-cbg.de
DOI 10.1016/j.neuron.2008.09.020

SUMMARY

Basal (intermediate) progenitors are the major source of neurons in the mammalian neocortex. The molecular machinery governing basal progenitor biogenesis is unknown. Here, we show that the zinc-finger transcription factor *Insm1* (insulinoma-associated 1) is expressed specifically in progenitors undergoing neurogenic divisions, has a panneurogenic role throughout the brain, and promotes basal progenitor formation in the neocortex. Mouse embryos lacking *Insm1* contained half the number of basal progenitors and showed a marked reduction in cortical plate radial thickness. Forced premature expression of *Insm1* in neuroepithelial cells resulted in their mitosis occurring at the basal (rather than apical) side of the ventricular zone and induced expression of the basal progenitor marker Tbr2. Remarkably, these cells remained negative for Tis21, a marker of neurogenic progenitors, and did not generate neurons but underwent self-amplification. Our data imply that Insm1 is involved in the generation and expansion of basal progenitors, a hallmark of neocortex evolution.

INTRODUCTION

A hallmark of mammalian brain evolution is the expansion of the cerebral cortex. The concomitant increase in cortical neurons largely reflects an increase in the number of neuron-generating (neurogenic) divisions of progenitor cells (PCs). Two principal parameters determine how many of these divisions occur during cortical neurogenesis: (1) how often a given PC undergoes neurogenic divisions and (2) how many PCs capable of undergoing neurogenic division (neuronal PCs) are formed (Caviness et al., 1995; Dehay and Kennedy, 2007; Huttner and Kosodo, 2005; Kriegstein et al., 2006; Rakic, 1995).

Neuronal PCs in the developing mammalian cerebral cortex can be classified into two principal groups depending on where mitosis occurs. One group comprises the PCs that divide at the ventricular surface (or very close to it). These include the neuroepithelial (NE) cells, the primary PCs of the central nervous system (CNS) (Götz and Huttner, 2005), and the PCs they transform into with the onset of neurogenesis, the radial glial cells (Kriegstein and Götz, 2003) and the short neural precursors (Gal et al., 2006). As apical-basal cell polarity is a characteristic feature of these PCs (Götz and Huttner, 2005) and the ventricular surface corresponds to their apical plasma membrane, these PCs will be collectively referred to as APs (Haubensak et al., 2004; Konno et al., 2008).

The other group comprises the PCs that divide away from the ventricular surface, in the basal region of the ventricular zone (VZ) and in the adjacent subventricular zone (SVZ). These PCs have been referred to as basal progenitors (BPs) (Haubensak et al., 2004) or non-surface-dividing PCs (to indicate the site of their mitosis) (Miyata et al., 2004) or as intermediate PCs (to indicate their place in the lineage from APs to neurons) (Kriegstein et al., 2006; Noctor et al., 2004; Pontious et al., 2008). Importantly, by dividing in an abventricular location, BPs serve as a means of substantially increasing the number of mitoses that can occur per unit segment of ventricular wall, as compared to a situation in which mitoses are confined to the ventricular surface (Haubensak et al., 2004; Kriegstein et al., 2006; Pontious et al., 2008; Smart, 1972b).

Consistent with this, BPs are a characteristic feature of mammals (as opposed to other vertebrates); are most abundant in the telencephalon, the part of the mammalian CNS with the greatest production of neurons; and are the source of most cortical neurons (Haubensak et al., 2004; Pontious et al., 2008). Moreover, the expansion of the mammalian cerebral cortex is associated with an increase in BPs relative to APs (Rakic, 2003; Smart et al., 2002; Tarabykin et al., 2001). This increase is thought to reflect the capacity of BPs to self-expand their population by symmetric division (Kriegstein et al., 2006; Pontious et al., 2008), with the founder BPs arising from APs (Attardo et al., 2008; Miyata et al., 2004).

A central question of cortical neurogenesis therefore is: Which molecules govern the production of BPs? While perturbation of proteins implicated in apical-basal polarity (Cappello et al., 2006) and cleavage plane orientation (Buchman and Tsai, 2007; Konno et al., 2008; Morin et al., 2007) can result in mitoses

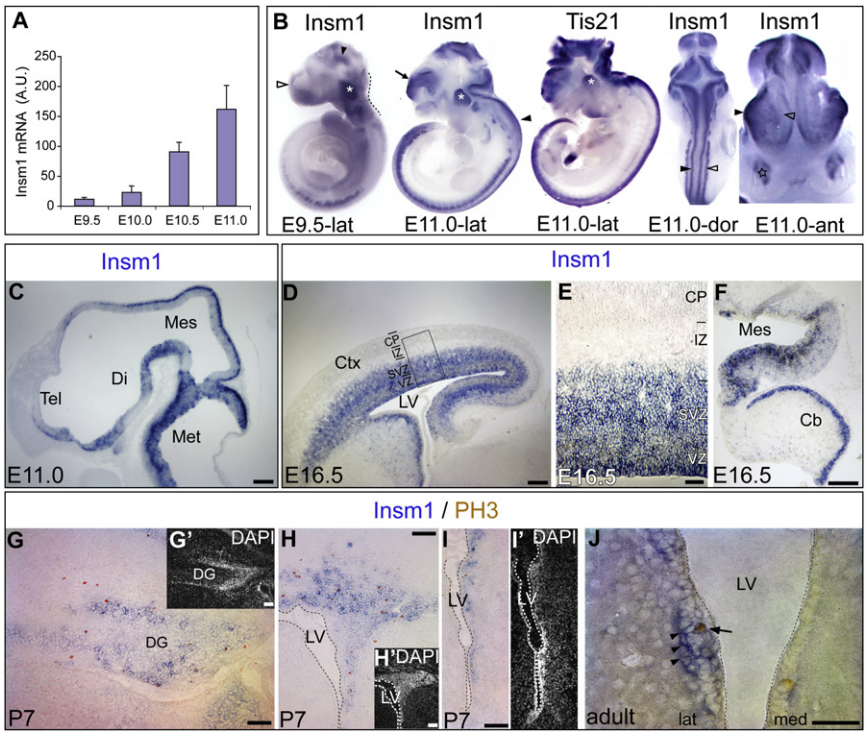

Figure 1. Mouse *Insm1* mRNA Expression Correlates with Neurogenesis throughout the Embryonic and Adult CNS

(A) *Insm1* mRNA levels (in arbitrary units [A.U.]) in the E9.5–E11.0 dorsal telencephalon (dTel) as revealed by microarray analysis. Data are the mean of three (E9.5–E10.5) or two (E11.0) independent samples; bars indicate SD (E9.5–E10.5) or the variation of the individual values from the mean (E11.0).

(B) Whole-mount in situ hybridization (ISH) for *Insm1* and *Tis21* mRNAs of E9.5–E11.0 mouse embryos. Lat, lateral view; dor, dorsal view; ant, anterior view. White asterisks, trigeminal ganglion; white and black arrowheads in E9.5-lat, telencephalon and ventral midbrain, respectively; dashed line, mid-hindbrain boundary; arrow and arrowhead in E11.0-lat, telencephalic vesicle and spinal cord, respectively; black and white arrowheads in E11.0-dor, spinal cord and dorsal root ganglia, respectively; black and white arrowheads in E11.0-ant, ventrolateral and dTel, respectively; star in E11.0-ant, olfactory placode.

(C–F) ISH for *Insm1* mRNA on sagittal cryosections of E11.0–E16.5 mouse brains. Boxed region in (D) is shown at higher magnification in (E). Note that (D)–(F) show cryosections from *Tis21*-GFP knockin mice that had also been subjected to immunoperoxidase staining for GFP. Di, diencephalon; Mes, mesencephalon; Met, metencephalon; Ctx, cortex; CP, cortical plate; IZ, intermediate zone; LV, lateral ventricle; Cb, cerebellum. Scale bars = 200 μm in (C), (D), and (F) and 50 μm in (E).

(G–J) ISH on coronal cryosections of postnatal (P7) and adult (4 months) brains for *Insm1* mRNA (blue, [G]–[J]) in combination with phosphohistone H3 (PH3) immunoperoxidase (brown, [G]–[J]) and DAPI staining (G′, H′, and I′). Arrowheads in (J) indicate *Insm1*-expressing cells, one of which is in mitosis (arrow). DG, dentate gyrus; LV, lateral ventricle; lat, lateral; med, medial. Scale bars = 100 μm in (G)–(I) and 50 μm in (J).

occurring in an abventricular location, the molecular machinery that is involved in the physiological transition from APs to BPs is unknown. Using both loss- and gain-of-function analyses, we report here that the transcription factor Insm1 (insulinoma-associated 1) (Gierl et al., 2006; Goto et al., 1992; Lan et al., 1994; Wildner et al., 2007; Xie et al., 2002) has a panneurogenic role throughout the brain and, in the neocortex, is a master regulator of BP biogenesis.

RESULTS

Insm1 Expression Correlates with Neurogenesis throughout the Nervous System

To identify candidate genes involved in the switch of neural PCs from proliferative to neurogenic divisions, we performed genome-wide gene expression profiling of the E9.5–E11.0 mouse dorsal telencephalon (dTel) at 12 hr intervals. A particularly interesting candidate gene whose expression in the CNS showed a striking correlation with the onset of neurogenesis and which appeared to be specifically expressed in neural PCs was insulinoma-associated 1 (*Insm1*, *IA-1*), a zinc-finger transcription factor identified in human pancreatic β cell tumors (Goto et al., 1992). Specifically, by microarray analysis, *Insm1* mRNA was barely detectable in the dTel until E10.0 but showed a steep increase in expression levels at E10.5 and E11.0 (Figure 1A). Whole-mount in situ hybridization (ISH) revealed the presence of *Insm1* mRNA throughout the central (Figure 1B) and peripheral (see Figure S1 available online) nervous system (Gierl et al., 2006; Wildner et al., 2007). *Insm1* expression in the CNS reflected the known gradients of neurogenesis, i.e., it was first detectable in the midbrain-hindbrain region (Figure 1B, E9.5-lat, black arrowhead and line) and then spread caudally throughout the spinal cord (Figure 1B, E11.0-lat and E11.0-dor, black arrowheads) and rostrally to the telencephalon (Figure 1B, E11.0-lat, arrow) in a ventral-to-dorsal fashion (Figure 1B, E11.0-ant, black and white arrowheads, respectively). Importantly, the temporal and spatial expression pattern of *Insm1* in the CNS was essentially indistinguishable from that of *Tis21* (Figure 1B), a panneurogenic PC marker (Haubensak et al., 2004; Iacopetti et al., 1999).

ISH on cryosections corroborated the expression of *Insm1* in the CNS in correlation with the gradients of neurogenesis and revealed that its expression was confined to the PC layers (Figure 1C). Notably, in the developing neocortex, *Insm1* mRNA was abundant in both the VZ and SVZ (Figures 1D and 1E), i.e., the two neuronal PC-containing layers. Interestingly, at later stages of development, *Insm1* expression specifically occurred in brain areas showing characteristic patterns of neurogenesis, such as (1) the external granule cell layer of the developing cerebellum (Figure 1F), (2) the dentate gyrus of the postnatal hippocampus (Figures 1G and 1G′), and (3) the wall of the lateral ventricle at postnatal day P7 (Figures 1H–1I′), where it persisted into adulthood (Figure 1J). Taken together, our expression data suggest that Insm1 is a panneurogenic transcription factor.

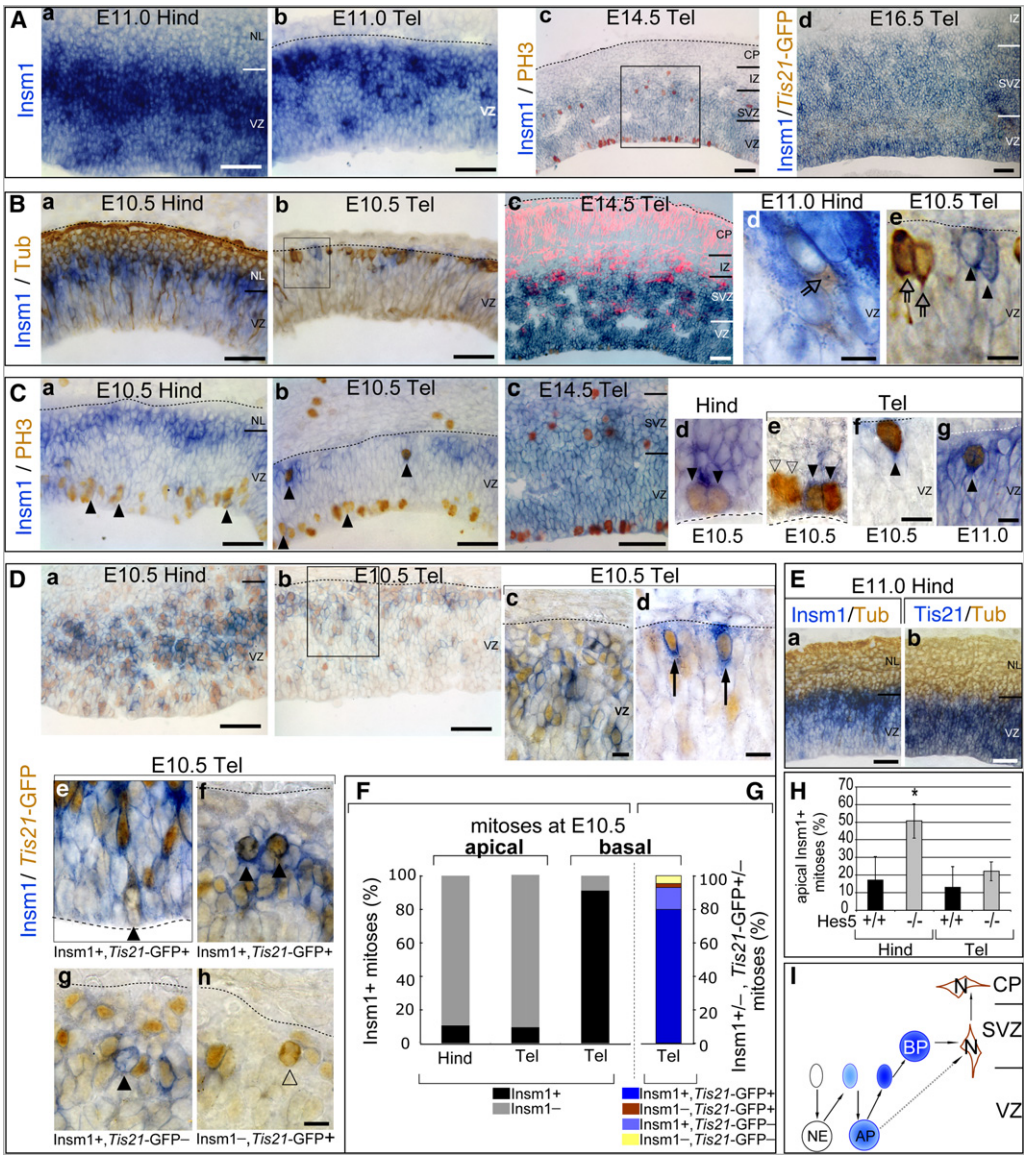

Figure 2. *Insm1* mRNA Is Expressed in Neurogenic Progenitor Cells

(A–E) ISH for *Insm1* or *Tis21* (blue) combined with immunoperoxidase (brown) on cryosections of E10.5–E16.5 mouse brain. Ventricular surface is down (dashed lines); basal lamina is indicated by dotted lines. Hind, hindbrain; IZ, intermediate zone; NL, neuronal layer; CP, cortical plate. Scale bars = 50 μm unless otherwise indicated.

(A) Staining for PH3 (Ac) and GFP ([Ad], *Tis21*-GFP knockin mouse). Boxed region in (Ac) is shown at higher magnification in (Cc).

(B) Staining for βIII-tubulin (Tub); (Bc) shows immunofluorescence (IF) (red) rather than immunoperoxidase. Boxed region in (Bb) is shown at higher magnification in (Be). Arrows, newborn neurons; arrowheads, *Insm1*-expressing cells. Scale bars in (Bd) and (Be) = 10 μm.

(C) Staining for PH3. Black arrowheads, mitotic *Insm1*-expressing apical progenitors (APs) and basal progenitors (BPs); white arrowheads, mitotic *Insm1*-negative APs. (Cd) and (Ce) and (Cf) and (Cg) show APs and BPs, respectively, at higher magnification. Scale bars = 10 μm in (Cf) (for [Cd]–[Cf]) and in (Cg).

(D) Staining for GFP (*Tis21*-GFP knockin mouse). Boxed region in (Db) is shown at higher magnification in (Dc). Arrows in (Dd) indicate *Insm1*- and *Tis21*-GFP-expressing cells. Black arrowheads in (De)–(Dh) indicate an *Insm1*- and *Tis21*-GFP-expressing mitotic AP (De), *Insm1*- and *Tis21*-GFP-expressing mitotic BPs (Df), and an *Insm1*-expressing but *Tis21*-GFP-negative mitotic BP (Dg); white arrowhead indicates a *Tis21*-GFP-expressing but *Insm1*-negative mitotic BP (Dh). Mitotic cells were identified by PH3 IF and DAPI staining (not shown). Scale bars = 10 μm in (Dc), (Dd), and (Dh) (for [De]–[Dh]).

(E) Staining for βIII-tubulin.

(F and G) Quantitation of mitotic APs and BPs (identified by PH3 IF) expressing *Insm1* (F) and *Insm1* and/or *Tis21*-GFP ([G], *Tis21*-GFP knockin mouse), as indicated. More than 500 cells were counted for each condition in (F), and 126 cells were counted in (G).

(H) Quantitation of mitotic APs (identified by PH3 staining) expressing *Insm1* in wild-type (+/+) and *Hes5* knockout (−/−) E10.5 hindbrain (Hind) and dTel. Data are the mean of three embryos; bars indicate SD. *$p < 0.01$.

(I) Cartoon summarizing *Insm1* mRNA expression (blue) and its increase from AP to BP in the dTel at the onset of neurogenesis. NE, neuroepithelial cells undergoing proliferative, but not yet neurogenic, division; N, newborn neurons; CP, cortical plate; VZ, ventricular zone; SVZ, subventricular zone.

Insm1 Is Expressed in Neurogenic APs and BPs

Closer examination by ISH of the distribution of *Insm1* mRNA in the VZ at the onset of neurogenesis revealed the highest levels of expression in cell bodies located at the basal side of the VZ (Figures 2Aa and 2Ab). This pattern, together with the restriction of *Insm1* expression to the PC-containing layers in correlation with neurogenesis (Figure 1), would be consistent with either expression in neurogenic PCs, transient expression in newborn neurons, or both. We used ISH in combination with immunohistochemistry on E10.5–E11.0 hindbrain and E10.5–E16.5 telencephalon to determine which was the case.

Counterstaining for the early neuronal marker βIII-tubulin showed that *Insm1* mRNA was not detected in the neuronal layers and/or cortical plate (Figures 2Ba, 2Bc, and 2Ea). Moreover, the newborn neurons that either were found within the VZ (Figure 2Bd, arrow) or were forming the first neuronal layer (Figures 2Bb and 2Be, arrows) also lacked *Insm1* mRNA.

Counterstaining for the mitotic marker phosphohistone H3 (PH3) showed that *Insm1* mRNA was detected in both (1) PCs dividing at the apical side of the VZ (NE cells, radial glial cells, and short neural precursors [Pontious et al., 2008], collectively referred to as APs [Haubensak et al., 2004]) and (2) PCs dividing in the basal region of the VZ and, at later stages of neurogenesis in the telencephalon, in the SVZ (Haubensak et al., 2004; Miyata et al., 2004; Noctor et al., 2004) (collectively referred to as BPs [Haubensak et al., 2004]) (Figures 2Ca–2Cc; see also Figure 2Ac). The vast majority of mitotic BPs were *Insm1* positive throughout neurogenesis (Figure 2F; Figures 2Cb, 2Cc, 2Cf, and 2Cg). By contrast, the proportion of *Insm1*-positive APs was small at the onset of neurogenesis (Figure 2F; Figures 2Cd and 2Ce) and appeared to increase with its progression (compare Figures 2Cb and 2Cc). We noticed that at the onset of neurogenesis, *Insm1* mRNA levels were consistently lower in the *Insm1*-positive mitotic APs than mitotic BPs (Figure 2Cb; see also Figure 2I). Taken together, these observations suggested that *Insm1* is specifically expressed in neurogenic PCs rather than newborn neurons (Figure 2I).

To examine this further, we compared the expression of *Insm1* with that of the panneurogenic marker Tis21 at the single-cell level, taking advantage of the *Tis21*-GFP knockin mouse line (Haubensak et al., 2004), in which GFP is expressed under the control of the *Tis21* promoter. Counterstaining for *Tis21*-GFP at the onset of neurogenesis, when individual neurogenic PCs can be more easily discerned from surrounding cells than at later stages, revealed an almost complete overlap with *Insm1* expression in both interphase (Figure 2Da) and mitotic (Figure 2De) APs as well as interphase (Figure 2Dd) and mitotic (Figure 2Df) BPs. Specifically, quantification of mitotic BPs (Figure 2G) at the onset of neurogenesis (E10.5) showed that the vast majority (80%) were positive for both *Insm1* mRNA and *Tis21*-GFP, with only a minority expressing either *Insm1* alone (13%; Figure 2Dg), *Tis21*-GFP alone (2%; Figure 2Dh), or neither marker (5%). Consistent with this, the *Insm1* and *Tis21* expression patterns with regard to PC versus neuronal layers, as revealed by ISH, were very similar (Figure 2E). We conclude that Insm1, like Tis21, is a panneurogenic PC marker (Figure 2I).

Insm1 Expression Is Controlled by Positive and Negative Transcriptional Regulators of Neurogenesis

The levels of *Insm1* mRNA were found to be controlled by *Hes* genes and proneural genes (for details, see Supplemental Results and Discussion and Figures S2 and S3). In particular, in the E10.5 hindbrain of *Hes5* knockout mice, a much greater proportion (≈50%) of APs than normal showed *Insm1* expression (Figure 2H).

Ablation of *Insm1* Reduces SVZ and Cortical Plate Radial Thickness

To directly investigate the role of Insm1 in neurogenesis, we analyzed *Insm1* null mouse embryos, in which the role of Insm1 has thus far been investigated with regard to the development of the endocrine pancreas and sympathoadrenal system (Gierl et al., 2006; Wildner et al., 2007). Given the higher level of *Insm1* mRNA in BPs than in APs (Figure 2) and its expression in almost all BPs (Figures 2F and 2G), we concentrated on neurogenesis in the dTel, where the majority of neurons are thought to be generated by BPs (Haubensak et al., 2004; Pontious et al., 2008). *Insm1* ablation leads to embryonic lethality starting at E11.5 (Gierl et al., 2006) (see Experimental Procedures), and the latest embryonic stage at which we could (rarely) obtain embryos was E16.5. Therefore, most of our analyses of the developing *Insm1* null neocortex were carried out at E13.5–E14.5, and the latest developmental stage analyzed was E16.5.

Whereas E13.5–E14.5 *Insm1* null brains did not show any striking abnormalities with regard to gross anatomical structure as observed macroscopically (data not shown), immunohistochemical analysis revealed a slight (albeit not statistically significant) reduction in the radial thickness of the E13.5–E14.5 dTel compared to either wild-type or heterozygous littermates (compare Figure 3A versus 3B and Figure 3G versus 3H and 3S). This reduction became greater by E16.5 (compare Figure 3I versus 3J and Figure 3K versus 3L and 3W) and affected predominantly the SVZ (Figures 3V and 3Z) and cortical plate (Figures 3T and 3X), as was also evident from staining for βIII-tubulin (compare Figure 3C versus 3D). Comparative quantitation of Tbr1-positive and DAPI-stained nuclei in the cortical plate at E13.5 revealed an essentially identical decrease in the *Insm1* knockouts (Figure S4), indicating that the reduction in the radial thickness of the cortical plate upon *Insm1* ablation was due to a reduction in neurons.

This reduction was not due to increased neuronal death. Immunofluorescence (IF) for activated caspase-3 (Figures S5C and S5D), a marker of apoptotic cells, or DAPI staining (Figures S5A and S5B; Figures 3K and 3L) did not reveal detectable cell death in the E14.5 and E16.5 *Insm1* null telencephalon. Together with the reduction in the radial thickness of the SVZ (Figures 3V and 3Z), the major site of neurogenesis (Haubensak et al., 2004; Pontious et al., 2008), these data suggested that the generation of cortical neurons in the mouse dTel was impaired in the absence of *Insm1*.

Ablation of *Insm1* Leads to Expansion of the VZ at the Expense of the SVZ

In contrast to the decrease in the radial thickness of the cortical plate (Figures 3T and 3X) and SVZ (Figures 3V and 3Z), the

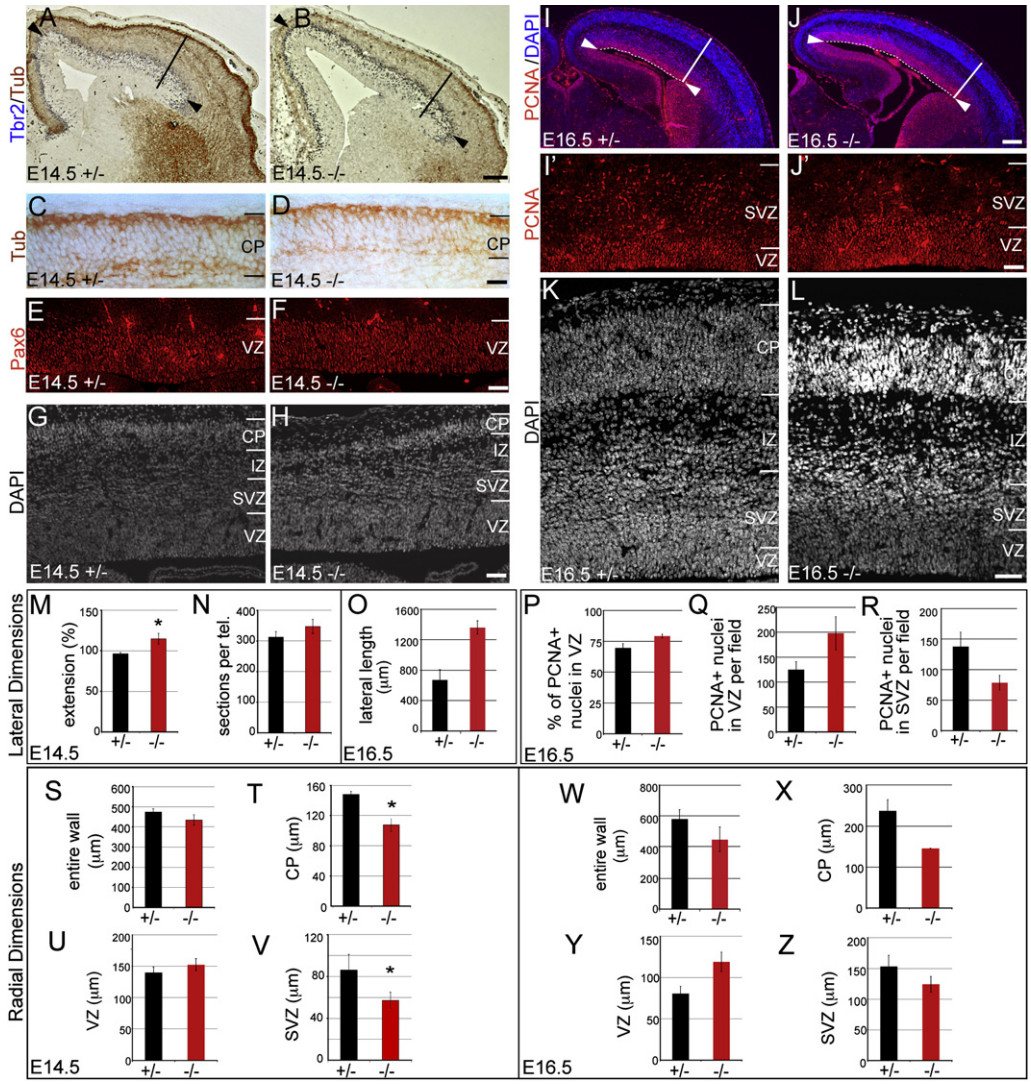

Figure 3. Reduction in SVZ and CP Thickness and Increase in VZ Thickness and Lateral Expansion of the Dorsal Telencephalon of *Insm1* Knockout Mouse Embryos

Cryosections of littermate wild-type, heterozygous (+/−, black bars), and homozygous (−/−, red bars) embryos were analyzed. As wild-type and heterozygous embryos were indistinguishable, only the results for heterozygous and homozygous embryos are shown. IZ, intermediate zone; CP, cortical plate. Scale bars = 200 μm in (B and J) and 50 μm in all other panels. +/− and −/− pairs are shown at the same magnification.

(A–H) E14.5.

(A and B) Overview; double immunoperoxidase for Tbr2 (blue, nickel enhancement) and βIII-tubulin (Tub) (brown). Arrowheads indicate the maximum lateral extension of the dTel in the image as revealed by Tbr2 immunostaining (see quantification in [M]). The lines indicate the position of the quantitations shown in (S)–(V) and the standard position of the lateral edges of the 20× and 40× images taken in this study.

(C and D) βIII-tubulin immunoperoxidase.

(E and F) Pax6 IF.

(G and H) DAPI staining.

(I–L) E16.5.

(I and J) Overview; PCNA IF (red) combined with DAPI staining (blue). Dashed lines and arrowheads indicate the lateral extension of the dTel at the ventricular surface (see quantification in [O]). Solid lines indicate the position of the quantitations shown in (W)–(Z) and the standard position of the lateral edges of the 20× and 40× images taken in this study.

(I′ and J′) PCNA IF in the VZ and SVZ at higher magnification.

(K and L) DAPI staining.

(M–O) Quantification of the lateral dimension of the dTel at E14.5 (M and N) and E16.5 (O).

(M) Lateral extension as determined from the distance between the tips of the arrowheads shown in (A) and (B). For each section along the rostrocaudal axis analyzed, data were first expressed as a percentage relative to wild-type (mean of three embryos), followed by calculation of the average percentage for all sections of a given embryo. Data are the mean of three embryos; bars indicate SD. *$p < 0.05$.

(N) Total number of sections required to cover the dTel (tel.). Data are the mean of three embryos; bars indicate SD.

radial thickness of the VZ in the *Insm1* null dTel was not reduced (Figure 3U) but actually increased, which was particularly evident at E16.5 (Figure 3Y). This was due to an increase in the number (rather than the proportion) of cycling cells in the VZ, as revealed by PCNA IF (Figures 3I′, 3J′, 3P, and 3Q). Interestingly, consistent with the decrease in the radial thickness of the SVZ (Figure 3Z), the number of PCNA-positive cells in the SVZ was reduced (Figure 3R), and this reduction largely corresponded to the increase in PCNA-positive cells in the VZ (Figure 3Q).

Remarkably, the *Insm1* null dTel exhibited not only a radially thicker VZ but also an expansion in the lateral dimension, which was greater at E16.5 than at E14.5 (compare Figure 3A versus 3B and Figure 3I versus 3J and 3M–3O). We conclude that ablation of *Insm1* impairs the formation of the SVZ, with a concomitant expansion of the VZ.

Ablation of *Insm1* Impairs the Generation of BPs

Given these changes in the VZ and SVZ upon *Insm1* ablation, we investigated APs and BPs in greater detail. IF for PH3 (Figures 4A and 4B) revealed a reduction in the number of mitotic BPs in the E13.5 and E14.5 *Insm1* null dTel to about half of that in wild-type and heterozygous littermates (Figure 4D and data not shown), whereas mitotic APs showed a small, albeit not statistically significant, increase (Figure 4C). Similar results were obtained when APs and BPs were quantitated at E11.5 (data not shown) and E16.5 (Figures 4M–4P).

We sought to corroborate the reduction in BPs upon ablation of *Insm1* by immunostaining for Tbr2 (Figures 4E and 4F), which is expressed, along with *Insm1* (Figures 4I and 4J), in almost all BPs (Englund et al., 2005) (Figure 4K). Indeed, an essentially identical reduction in mitotic BPs was observed when Tbr2-positive basal mitoses were quantified (Figure 4H). Analysis of Tbr2-positive interphase nuclei (rather than Tbr2-positive basal mitoses) also revealed a reduction for the *Insm1* null dTel (Figure 4L). Interestingly, we observed a decrease very similar to that in Tbr2-positive basal mitoses (Figure 4H) when, instead of examining all apical mitoses in the *Insm1* null dTel (Figure 4C), we counted only the Tbr2-positive apical mitoses (Figure 4G). The latter constitute a small subpopulation of all apical mitoses (Englund et al., 2005) and presumably constitute APs that generate BPs. Together with the observation that there was no increased cell death in the *Insm1* null cortical wall (Figure S5), our data indicate that *Insm1* ablation reduces the generation of BPs throughout neurogenesis.

Both Deep Layer and Upper Layer Neurons Are Reduced in *Insm1* Null Neocortex

Given these observations, it was important to investigate the abundance of neurons in the various layers of the *Insm1* null neocortex, as deep layer and upper layer neurons are generated during the early and late stages of neurogenesis, respectively (Molyneaux et al., 2007). The overall reduction in radial thickness of the E16.5 cortical plate upon *Insm1* ablation, as revealed by IF for the general marker of young neurons βIII-tubulin (Figures 4Q and 4R), was due to a reduction in both deep layer neurons, identified by Tbr1 IF (Figures 4U and 4V; see also Figure S4) (Englund et al., 2005), and upper layer neurons, identified by Brn1 IF (Figures 4S and 4T) (Molyneaux et al., 2007). IF for another marker of deep layer neurons, Foxp2 (Molyneaux et al., 2007), revealed a reduction similar to that observed for Tbr1 (Figures 4W and 4X). *Insm1* ablation did not result in a premature switch of neocortical PCs from the neuronal to the glial lineage, as revealed by CD44 and nestin IF of E16.5 *Insm1* null neocortex (for details, see Supplemental Results and Discussion and Figure S6). These data indicate that, consistent with the reduction in BPs at early as well as late stages of neurogenesis, both deep layer and upper layer neuron production are decreased in the developing *Insm1* null neocortex.

Insm1 Ablation Leads to Reduced Neurogenesis in Brain Regions Other Than the Neocortex

Given that (1) *Insm1* ablation reduces neurogenesis and BPs in the developing neocortex (Figure 3; Figure 4) and (2) *Insm1* expression occurs throughout the developing brain in the VZ and (when present) SVZ in correlation with neurogenesis (Figure 1; Figure 2), it was of interest to investigate whether *Insm1* ablation impaired neurogenesis in brain regions other than the dTel. In both the developing hindbrain (Figures 4Ya and 4Yb) and midbrain (Figures 4Za and 4Zb), where neurogenesis occurs earlier than in the dTel and BPs are very rare (Haubensak et al., 2004), *Insm1* ablation resulted in a reduction in the thickness of the neuronal layer as revealed by βIII-tubulin IF at E11.5. In contrast, Pax6 IF did not reveal any obvious changes in the hindbrain and midbrain VZ at this early developmental stage (Figures 4Y and 4Z). For other brain regions, see Supplemental Results and Discussion and Figure S7.

Forced Premature *Insm1* Expression Increases the Occurrence of Tbr2-Positive Basal Mitoses at the Expense of Apical Mitoses

Given that *Insm1* is necessary for the generation of BPs, we investigated whether it is sufficient to increase the occurrence of

(O) Lateral extension as determined from the distance between the tips of the arrowheads shown in (I) and (J). Data are the mean of three (+/−) and two (−/−) embryos (at least 12 cryosections per embryo); bars indicate SD (+/−) or the variation of the individual values from the mean (−/−).
(P–R) Quantification of PCNA-positive nuclei in the VZ and SVZ at E16.5 as determined after IF in combination with DAPI staining in rectangular fields (20×), each corresponding to 110 μm of ventricular surface. Data are the mean of three (+/−) and two (−/−) embryos; bars indicate SD (+/−) or the variation of the individual values from the mean (−/−).
(P) Proportion of DAPI-stained nuclei in the VZ that are PCNA positive.
(Q and R) Number of PCNA-positive nuclei per field in the VZ (Q) and SVZ (R).
(S–Z) Quantification of the radial dimensions of the dTel at E14.5 (S–V) and E16.5 (W–Z).
(S–V) Radial thickness of the entire cortical wall (S), the cortical plate (T), the VZ (U), and the SVZ (V), determined at the position of the lines shown in (A) and (B). Data are the mean of five (+/−) and three (−/−) embryos; bars indicate SD. *$p < 0.05$.
(W–Z) Radial thickness of the entire cortical wall (W), the cortical plate (X), the VZ (Y), and the SVZ (Z), determined at the position of the lines shown in (I) and (J). Data are the mean of three (+/−) and two (−/−) embryos; bars indicate the variation of the individual values from the mean.

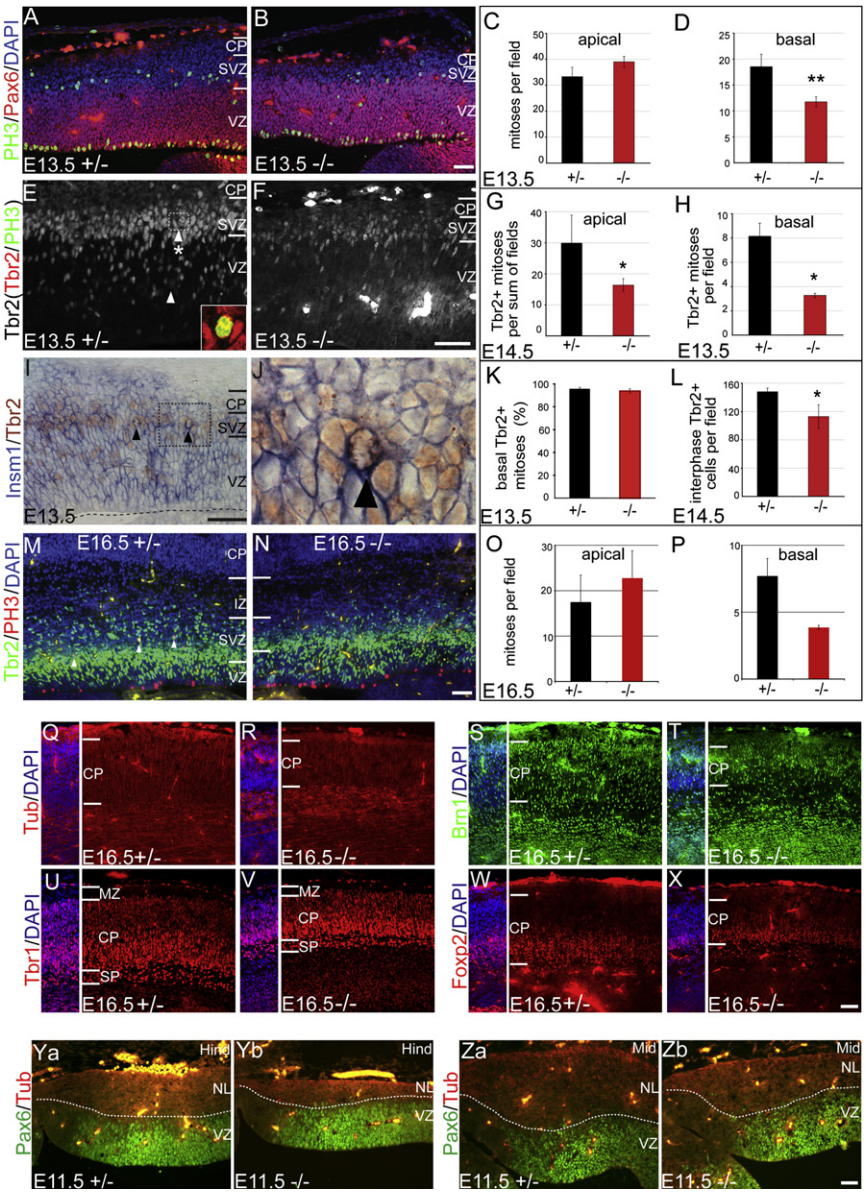

Figure 4. Reduction in BPs and Neurons of All Cortical Layers in the Dorsal Telencephalon of *Insm1* Knockout Mouse Embryos

Cryosections of littermate wild-type, heterozygous (+/−, black bars), and homozygous (−/−, red bars) embryos were analyzed (except for [I] and [J]). As wild-type and heterozygous embryos were indistinguishable, only the results for heterozygous and homozygous embryos are shown. IZ, intermediate zone; SP, subplate; CP, cortical plate; MZ, marginal zone. Scale bars = 50 μm. +/− and −/− pairs are shown at the same magnification.

(A and B) PH3 (green) and Pax6 (red) double IF combined with DAPI staining (blue) at E13.5.

(C and D) Number of mitotic APs (C) and BPs (D) at E13.5 as revealed by PH3 IF (field = 20× image). Data are the mean of four (+/−) and three (−/−) embryos; bars indicate SD. **$p < 0.01$.

(E and F) Tbr2 IF at E13.5. Arrowheads indicate Tbr2-expressing mitotic BPs (identified by PH3 IF). Inset in (E): double IF for Tbr2 (red) and PH3 (green) of the cell indicated by the asterisk.

(G and H) Number of Tbr2-expressing mitotic APs at E14.5 ([G], sum of 12 fields = 20× images) and BPs at E13.5 ([H], field = 40× image), as revealed by double IF for PH3 and Tbr2. Data are the mean of five (+/−) and three (−/−) embryos for apical mitoses and four (+/−) and two (−/−) embryos for basal mitoses; bars indicate SD or the variation of the individual values from the mean. *$p < 0.02$.

(I and J) ISH for *Insm1* (blue) combined with staining for Tbr2 (brown) on cryosections of E13.5 dTel of NMRI mice. The boxed region in (I) is shown at higher magnification in (J). Arrowheads indicate *Insm1*- and Tbr2-expressing BPs in mitosis as revealed by DAPI staining (not shown). Dashed line, ventricular surface.

(K) Proportion of mitotic BPs (identified by PH3 IF) expressing Tbr2 at E13.5. Data are the mean of two embryos; bars indicate the variation of the individual values from the mean.

(L) Number of Tbr2-expressing cells in interphase at E14.5 as revealed by Tbr2 IF, determined for each image in a rectangular field corresponding to 123 μm of ventricular surface. Data are the mean of six (+/−) and three (−/−) embryos; bars indicate SD. *$p < 0.01$.

(M and N) Tbr2 (green) and PH3 (red) double IF combined with DAPI staining (blue) at E16.5. Arrowheads indicate mitotic BPs, essentially all of which are Tbr2 positive.

(O and P) Number of apical (O) and basal (P) mitoses at E16.5 as revealed by PH3 IF (field = 20× image). Data are the mean of three (+/−) and two (−/−) embryos; bars indicate SD (+/−) or the variation of the individual values from the mean (−/−).

(Q–X) βIII-tubulin ([Q and R]; Tub, red), Brn1 ([S and T]; green), Tbr1 ([U and V]; red), and Foxp2 ([W and X]; red) IF at E16.5, combined with DAPI staining (blue) as shown in the left segment of each panel.

(Y and Z) Pax6 (green) and βIII-tubulin (red) double IF in the ventral hindbrain (Hind, [Ya and Yb]) and ventral midbrain (Mid, [Za and Zb]) at E11.5. Dashed lines indicate the boundary between the VZ and the neuronal layers. Note the reduction in the radial thickness of the neuronal layers in the *Insm1* knockout.

basal mitoses. For this purpose, we carried out forced expression of *Insm1* in the dTel of E10.5 NMRI mice, i.e., at the onset of neurogenesis. Specifically, a plasmid driving *Insm1* expression from a constitutive promoter was electroporated into NE cells of embryos ex utero, followed by whole-embryo culture (WEC) for 24 hr. This in vitro system is known to allow embryonic development, and neurogenesis in particular, to proceed in a manner indistinguishable from that in utero (Calegari and Huttner, 2003). Moreover, we observed no significant apoptosis using this system, either in the control condition or upon any of the forced *Insm1* expressions described below (data not shown).

Upon electroporation of the E10.5 dTel, approximately one-third of NE cells are known to express the transgene (Osumi and Inoue, 2001), which was also observed in the present study when analyzing GFP expression from a reporter plasmid. Consistent with this, ISH revealed that upon forced *Insm1*

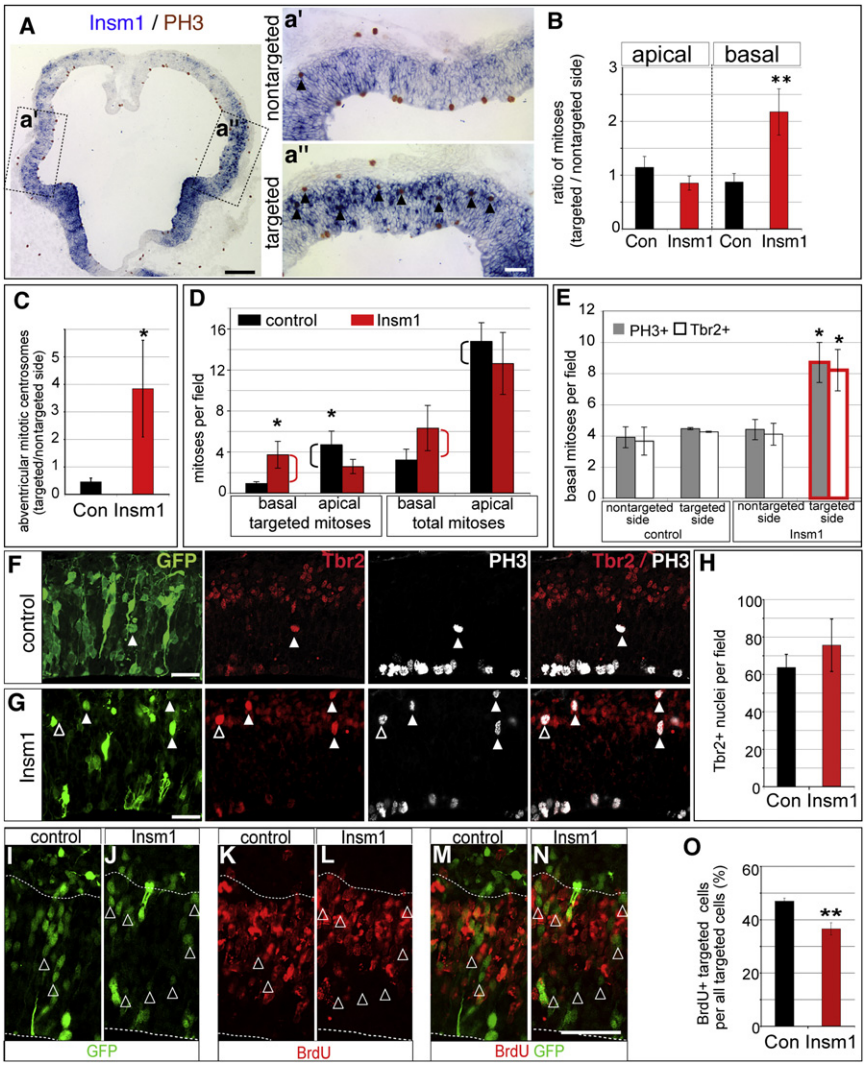

Figure 5. Forced Premature *Insm1* Expression in the Dorsal Telencephalon Increases the Number of Tbr2-Positive Basal Mitoses at the Expense of Apical Mitoses and Reduces Cell-Cycle Progression

dTel neuroepithelium of E10.5 NMRI mouse embryos was electroporated with a mixture of either empty plasmid (A–D) or nonexpressing *Insm1* plasmid (E–O) and GFP expression plasmid (control; Con, black bars) or *Insm1* expression plasmid and GFP expression plasmid (*Insm1*, red bars), followed by whole-embryo culture (WEC) for 24 hr without (A–H) or with (I–O) the presence of BrdU during the last 30 min and preparation of cryosections.

(A) An *Insm1*-electroporated embryo analyzed by ISH for *Insm1* (blue) combined with PH3 staining (brown). The boxed regions show, at higher magnification, the nontargeted side (Aa′) and the targeted side (Aa″). Arrowheads indicate mitotic BPs. Scale bars = 200 μm in (A) and 50 μm in (Aa″).

(B) Quantitation of apical and basal mitoses as revealed by PH3 staining. Data are expressed as the ratio of the targeted side to the corresponding nontargeted side and are the mean of four embryos each; bars indicate SD. **$p < 0.001$.

(C) Quantitation of centrosomes in mitotic BPs as revealed by analysis of the basal two-thirds of the VZ (rectangular field corresponding to 96 μm of ventricular surface per image) after DAPI staining and γ-tubulin IF. Data are expressed as the ratio of the targeted side to the corresponding nontargeted side and are the mean of three embryos each; bars indicate SD. *$p < 0.03$.

(D) Quantitation of total and targeted (GFP-positive) apical and basal mitoses of the targeted side as revealed by PH3 and GFP double IF (field = 40× image). Data are the mean of four (control) and three (Insm1) embryos; bars indicate SD. *$p < 0.02$ (basal); *$p < 0.05$ (apical). Brackets indicate the Insm1-induced gain in basal mitoses (red) and the loss in apical mitoses (black) in targeted cells.

(E) Comparison of total (gray bars) and Tbr2-positive (white bars) basal mitoses as revealed by PH3 and Tbr2 double IF (field = 40× image). Data are the mean of two (control) and three (Insm1) embryos; bars indicate SD or the variation of the individual values from the mean. *$p < 0.01$.

(F and G) Triple IF of the targeted side for GFP (green), Tbr2 (red), and PH3 (white). Arrowheads indicate targeted (GFP-positive, white) and nontargeted (GFP-negative, black) basal mitoses. Ventricular surface is down. Scale bars = 50 μm.

(H) Quantitation of Tbr2-positive interphase nuclei of the targeted side as revealed by Tbr2 IF (field = 40× image). Data are the mean of two (control) and three (Insm1) embryos; bars indicate SD or the variation of the individual values from the mean.

(I–N) BrdU incorporation of the targeted side as revealed by double IF for GFP ([I], [J], [M], and [N]; green) and BrdU ([K], [L], [M], and [N]; red). Arrowheads indicate BrdU-negative targeted cells. Ventricular surface is down (lower dashed lines); upper dashed lines indicate the basal boundary of the VZ. Scale bar = 50 μm.

(O) Quantitation of BrdU-labeled (BrdU+) targeted cells in the VZ as revealed by double IF for BrdU and GFP. Data are expressed as percentage of all targeted cells and are the mean of two (control) and three (Insm1) embryos; bars indicate SD or the variation of the individual values from the mean. **$p < 0.01$.

expression, a much greater proportion of NE cells than in the control condition showed robust *Insm1* mRNA levels (Figure 5A). In fact, the proportion of *Insm1* mRNA-positive NE cells observed upon electroporation at this very early stage of neurogenesis corresponded to that normally only observed at later stages (see Figure 2Bc). Hence, the forced *Insm1* expression actually constituted a premature expression with regard to most of the targeted NE cells. Forced premature expression of *Insm1* led to a more than 2-fold increase in the abundance of basal mitoses, as revealed by PH3 immunostaining (Figure 5B) or quantitation of abventricular mitotic centrosomes (Figure 5C). Apical mitoses were not increased but, if anything, slightly decreased (Figure 5B).

At E11.5, apical mitoses are much more abundant than basal mitoses (Haubensak et al., 2004), and so the gain in basal mitoses upon forced *Insm1* expression could correspond to the loss in apical mitoses. To investigate this, we restricted our analysis to the targeted cells, i.e., those that had actually received the *Insm1* expression plasmid, as indicated by the expression of the coelectroporated fluorescent reporter protein (GFP or

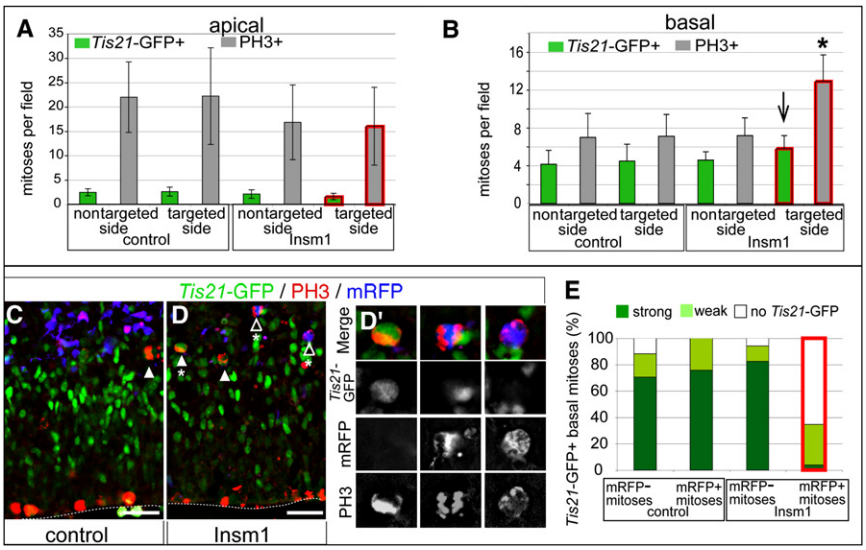

Figure 6. The Additional Basal Mitoses Induced by Forced Premature *Insm1* Expression Are *Tis21*-GFP Negative

dTel neuroepithelium of E10.5 *Tis21*-GFP knockin mouse embryos was electroporated with a mixture of either empty plasmid and mRFP expression plasmid (control) or *Insm1* expression plasmid and mRFP expression plasmid (Insm1, red outlines), followed by WEC for 24 hr and preparation of cryosections.

(A and B) Quantitation of strongly *Tis21*-GFP-positive (green bars) apical (A) and basal (B) mitoses in comparison to total mitoses (gray bars) as revealed by GFP and PH3 double IF (field = 40× image). Data are the mean of four (control) and six (Insm1) embryos; bars indicate SD. *$p < 0.02$. Note the lack of a significant increase in *Tis21*-GFP-positive basal mitoses upon forced expression of *Insm1* (arrow in [B]).

(C–D′) Triple IF of the targeted side for *Tis21*-GFP (green), PH3 (red), and mRFP (blue). White arrowheads indicate *Tis21*-GFP-positive basal mitoses; black arrowheads indicate *Tis21*-GFP-negative, targeted basal mitoses; asterisks indicate basal mitoses shown at higher magnification in (D′). Ventricular surface is down (dashed line). Scale bars = 50 μm.

(E) Analysis of *Tis21*-GFP expression in targeted (mRFP+) and nontargeted (mRFP−) basal mitoses (identified by PH3 IF). *Tis21*-GFP expression was detected by GFP IF and scored as absent (white), weak (light green), or strong (dark green; see top left panel in [D′] for an example). For each of the four cell populations, at least 17 mitoses were analyzed, and data are presented as percentage of the total number of mitoses.

mRFP). This revealed that forced *Insm1* expression reduced the targeted cells that divided apically to about half (Figure 5D), and this loss in apical mitoses matched the gain in basal mitoses (Figure 5D, black and red brackets, respectively).

The increased basal mitoses observed upon forced *Insm1* expression exhibited a characteristic feature of BPs, the expression of Tbr2 (Englund et al., 2005). Specifically, comparison with the total number of basal mitoses as revealed by PH3 IF showed that almost all of them were Tbr2 positive, as in the control situation (Figure 5E; see also Figures 5F and 5G). Analysis of interphase Tbr2-positive nuclei (rather than Tbr2-positive basal mitoses) also revealed a small, albeit not statistically significant, increase upon forced *Insm1* expression (Figure 5H; see also Figures 5F and 5G).

Forced Premature *Insm1* Expression Reduces Cell-Cycle Progression

Neurogenic PCs, and BPs in particular, lengthen their cell cycle (Calegari et al., 2005; Dehay and Kennedy, 2007; Takahashi et al., 1995b). Given the specific expression of *Insm1* in these PCs, we investigated whether Insm1 reduces their cell-cycle progression. *Insm1* along with a GFP reporter was electroporated into NE cells in the dTel of E10.5 NMRI mice, followed by WEC for 24 hr and BrdU labeling during the last 30 min of WEC (Figures 5I–5N). Forced *Insm1* expression led to a ≈20% decrease in the proportion of GFP-positive cells in the VZ that had incorporated BrdU (Figure 5O). This presumably reflected a lengthening of the cell cycle of the targeted PCs rather than cell-cycle withdrawal of a subpopulation of cells, as we did not observe an accumulation of βIII-tubulin-positive cells in the VZ (Figure S8) and 90% of the *Insm1*-electroporated cells in the VZ were found to be PCNA positive (data not shown; see also the PCNA IF below). We conclude that premature *Insm1* expression reduces cell-cycle progression of neural PCs. Consistent with this, we observed reduced proliferation of *Insm1*-transfected Neuro2a cells (Figure S9). This appears to be a conserved role of Insm1, as forced expression of *Insm1* in medaka nonneural PCs produces a similar effect (Candal et al., 2007).

The Additional Basal Mitoses Induced by Forced Premature *Insm1* Expression Are *Tis21*-GFP Negative

Two subpopulations of mitotic BPs can be distinguished, those showing Tis21 expression and those lacking it (Haubensak et al., 2004). Tis21-expressing BPs constitute up to 90% of all BPs in the dTel (Haubensak et al., 2004). We therefore investigated whether or not the additional basal mitoses observed upon forced *Insm1* expression showed Tis21 expression. Forced expression of *Insm1* in the dTel of E10.5 *Tis21*-GFP knockin embryos in WEC produced an effect very similar to that in NMRI mice (Figures 6A and 6B), causing an approximately 2-fold increase in the abundance of basal mitoses (Figure 6B). Remarkably, the increase in *Tis21*-GFP-positive basal mitoses was much less pronounced (Figure 6B, arrow) than the increase in the total number of basal mitoses (Figure 6B, asterisk), suggesting that forced *Insm1* expression preferentially induced the generation of Tis21-negative BPs.

This was further corroborated by separate analysis of the mitotic BPs originating from electroporated versus nonelectroporated NE cells, as revealed by the presence versus absence, respectively, of mRFP reporter fluorescence (Figures 6C–6D′). In the control condition, at least 90% of both mRFP-negative and mRFP-positive mitotic BPs showed either strong or weak *Tis21*-GFP expression (Figure 6E). Similarly, upon forced *Insm1* expression, >90% of the mRFP-negative mitotic BPs, i.e., those originating from nonelectroporated NE cells, showed *Tis21*-GFP expression (Figure 6E). By contrast, >60% of the mRFP-positive

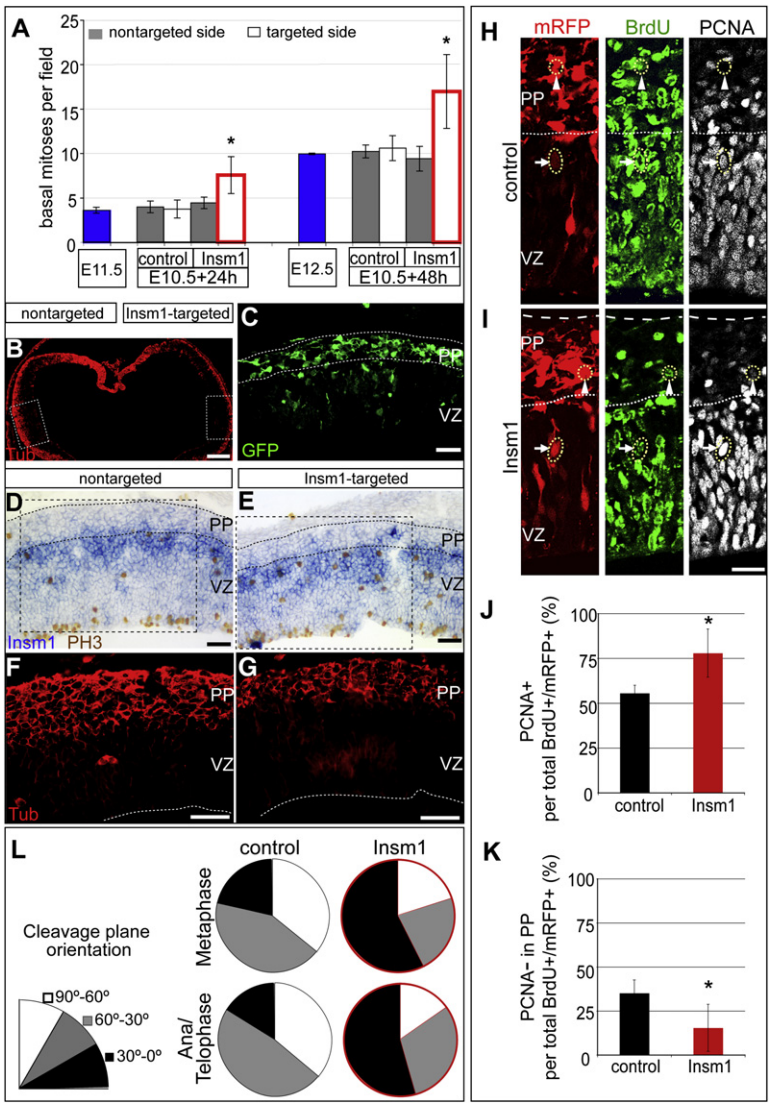

Figure 7. Forced Premature *Insm1* Expression Leads to an Accumulation of Basal Mitotic Cells at the Expense of Neurogenesis

dTel neuroepithelium of E10.5 NMRI mouse embryos was electroporated with a mixture of either empty plasmid (A–G) or nonexpressing *Insm1* plasmid (H–L) and GFP (A–G and L) or mRFP (H–K) expression plasmid (control), or *Insm1* expression plasmid (A–L) and GFP (A–G and L) or mRFP (H–K) expression plasmid (Insm1), followed by WEC for either 24 hr ([A] left) or 48 hr ([A] right, [B–L]), with a 1 hr BrdU pulse starting at 24 hr (H–K), and preparation of cryosections.

(A) Quantitation of basal mitoses at 24 hr and 48 hr as identified by PH3 staining (field = 40× image). Mitotic BPs from the dTel of E11.5 and E12.5 NMRI mouse embryos were quantitated for comparison (blue columns). Data are the mean of two (24 hr control, E12.5), three (Insm1, E11.5), and four (48 hr control) embryos each; bars indicate SD or the variation of the individual values from the mean. *$p < 0.05$.

(B–G) Combined ISH for *Insm1* ([D] and [E]; blue), immunoperoxidase for PH3 ([D] and [E]; brown), and double IF for GFP ([C], green) and βIII-tubulin ([B], [F], and [G]; Tub, red) of *Insm1*-electroporated embryos at 48 hr, with the nontargeted side serving as control. Dashed boxes in (B) indicate areas shown at higher magnification in (C)–(E); the dashed boxes in (D) and (E) indicate areas shown at higher magnification in (F) and (G). Ventricular surface is down (lower dashed lines in [F] and [G]); upper dashed lines in (C)–(E) indicate the boundaries of the preplate (PP). Scale bars = 200 μm in (B) and 50 μm in (C)–(G).

(H–K) Analysis of electroporated cells and their progeny (identified by mRFP), pulse-labeled with BrdU at 24 hr, for cell-cycle reentry at 48 hr (PCNA staining).

(H and I) Triple IF for mRFP (red), BrdU (green), and PCNA (white). Arrows indicate examples of mRFP-positive/BrdU-positive/PCNA-positive cells in the VZ; arrowheads indicate examples of mRFP-positive/BrdU-positive/PCNA-negative cells in the PP.

(J) Quantification of the proportion of mRFP- plus BrdU-positive cells in the cortical wall that are PCNA positive (field = 25× image). Data are the mean of six (control) and three (Insm1) embryos each (>100 mRFP- plus BrdU-positive cells per embryo were analyzed); bars indicate SD. *$p < 0.05$. Similar results were obtained when only cells in the VZ were scored (data not shown).

(K) Quantification of the proportion of mRFP- plus BrdU-positive cells in the PP that are PCNA negative (field = 25× image). Data are the mean of six (control) and three (Insm1) embryos each (>100 mRFP- plus BrdU-positive cells per embryo were analyzed); bars indicate SD. *$p < 0.05$. Similar results were obtained when cells were scored across the entire cortical wall (data not shown).

(L) Quantitation of the cleavage plane orientation at metaphase and anaphase/telophase, deduced from DAPI staining, of targeted basal mitoses, identified by intrinsic mRFP fluorescence and phosphovimentin IF, respectively. Cleavage plane orientation was assigned to one of three groups as indicated on the left; 0° corresponds to parallel to the ventricular surface. Data are from five (control, 28 metaphase and 25 anaphase/telophase cells) and three (Insm1, 40 metaphase and 33 anaphase/telophase cells) embryos.

mitotic BPs observed upon forced *Insm1* expression, i.e., those originating from electroporated NE cells, lacked *Tis21*-GFP expression, and *Tis21*-GFP expression in the remainder was weak (Figure 6E).

The increase in *Tis21*-GFP-negative basally dividing cells observed upon forced *Insm1* expression did not reflect a premature generation of astroglial PCs. Immunostaining for CD44 (Figure S10) and glial fibrillary acidic protein (data not shown) did not reveal any expression in the *Insm1*-electroporated dTel of E10.5 embryos subjected to WEC for 48 hr. Taking these data together, we conclude that Insm1 alone is sufficient to promote the generation of Tbr2-positive, but Tis21-negative, BPs in the mouse embryonic dTel.

The Additional BPs Induced by Forced Premature *Insm1* Expression Can Self-Amplify

The Tis21-negative subpopulation of APs is known to generate more PCs rather than neurons (Attardo et al., 2008; Haubensak et al., 2004; Noctor et al., 2004). Given that the additional BPs induced by forced *Insm1* expression were Tis21 negative (Figure 6), we investigated whether they would generate neurons or self-amplify. In the latter case, one would expect that upon

Table 1. Genes Whose Expression in the E13.5 Dorsal Telencephalon Is Decreased in the *Insm1* Knockout

Gene Symbol	Gene Name	Function	Expression in VZ/SVZ Progenitors	% of WT	p Value
Elavl4	Embryonic lethal, abnormal vision, *Drosophila*-like 4 (HuD)	RNA binding protein, neuronal progenitor differentiation	yes (weak)	74	0.023
Robo2	Roundabout homolog 2	Slit receptor, neuronal migration, neural progenitor proliferation versus differentiation[a]	yes[a]	63	0.023
Nhlh1	Nescient helix loop helix 1	Transcription factor, neuronal differentiation	yes (SVZ, strong)	62	0.027
Ebf3	Early B cell factor 3	Transcription factor, tumor suppressor, cell-cycle regulation	yes (weak)	73	0.028
Cntn2	Contactin 2	Cell adhesion	yes	61	0.034
Stat3	Signal transducer and activator of transcription 3	Signal transducer, transcriptional regulator, neural progenitor proliferation versus differentiation	yes (strong)	69	0.034
Abhd2	Abhydrolase domain containing 2	Membrane enzyme, brain tumor progression	yes (weak)	81	0.041
Myh9	Myosin, heavy polypeptide 9, nonmuscle (NMHC-IIA)	Motor protein	yes (weak)	83	0.044
Rbm9	RNA binding motif protein 9	Neuronal RNA splicing	yes (SVZ)	83	0.044
Net1	Neuroepithelial transforming gene 1	Rho-GEF	yes (weak)	80	0.045
Arhgef7	Rho guanine nucleotide exchange factor (GEF7)	Rho-GEF	yes (ubiquitous)	85	0.034
Mcart1	Mitochondrial carrier triple repeat 1	Mitochondrial metabolism	yes (ubiquitous)	76	0.044
Uba1	Ubiquitin-like modifier activating enzyme 1	Ubiquitination	yes (ubiquitous)	88	0.044
PLCb1	Phospholipase C, beta1	Signal transduction	not obvious (migrating neurons)	59	0.006
9030425E11Rik	Adipocyte adhesion molecule	Cell adhesion	not obvious (migrating neurons)	60	0.027
Nrp1	Neuropilin 1	Semaphorin/VEGF receptor, neuronal guidance, angiogenesis	not obvious (migrating neurons)	74	0.044
Acpl2	Acid phosphatase-like 2	Enzyme	not obvious (migrating neurons)	72	0.045
Lamb1-1	Laminin B1 subunit 1	Extracellular matrix	not obvious	72	0.006
St18	Suppressor of tumorigenicity 18	Transcription factor, tumor suppressor	not obvious	61	0.006
Dscam	Down syndrome cell adhesion molecule	Neuronal adhesion	not obvious	68	0.027
Kif5a	Kinesin family member 5A	Motor protein, axonal transport	not obvious	72	0.027
Rassf2	Ras association (RalGDS/AF-6) domain family 2	Ras effector, signal transduction, tumor suppressor	not obvious	69	0.027
Nefm	Neurofilament, medium polypeptide	Intermediate filament protein	not obvious	63	0.034
Snap91	Synaptosomal-associated protein 91 (AP180)	Clathrin adaptor, neuronal membrane traffic	not obvious	83	0.034
Crabp1	Cellular retinoic acid binding protein I	Retinoic acid metabolism	not obvious	64	0.040
Accn2	Amiloride-sensitive cation channel 2	Neuronal ion channel	ND	61	0.027
Gfpt1	Glutamine fructose-6-phosphate transaminase 1	Hexosamine metabolism	ND	82	0.028
Ipo9	Importin 9	Nuclear import	ND	81	0.044

dTel from E13.5 wild-type (WT) and homozygous *Insm1* knockout mouse embryos was subjected to microarray analysis. Genes whose expression in the *Insm1* knockout showed a change with an adjusted p value < 0.05 as compared to wild-type are listed. These 28 genes (other than *Insm1* itself), all of which showed a decreased level of expression (expressed as percentage of wild-type), were assigned to five groups depending on the pattern of

Insm1 electroporation and WEC for longer than 24 hr, additional BPs should continue to accumulate.

Upon electroporation of NE cells of E10.5 NMRI mice under control conditions and WEC for 48 hr, the abundance of mitotic BPs in the dTel was twice that observed after 24 hr (the standard length of WEC in the previous experiments in Figure 5 and Figure 6) and matched that of the corresponding stage of neurogenesis (E11.5 and E12.5) in utero (Figure 7A, blue columns). Forced expression of *Insm1* resulted in a doubling of the level of mitotic BPs not only after 24 hr but also after 48 hr (Figures 7A, 7D, and 7E). Concomitant with this, the accumulation of neurons in the preplate (Figure 7C) was markedly reduced compared to control (Figures 7B, 7F, and 7G).

We sought to obtain direct evidence that the additional BPs observed 48 hr after forced *Insm1* expression originated from Insm1-induced BPs generated during the first 24 hr of WEC. To this end, dTel of E10.5 embryos was electroporated with *Insm1* or under control conditions, using mRFP to identify the electroporated cells, and labeled after the first 24 hr of WEC for 1 hr with BrdU, followed by analysis after 48 hr of WEC. Specifically, we determined the proportion of the mRFP and BrdU double-positive cells that were PCNA positive after 48 hr of WEC, i.e., the proportion of PCs that originated from electroporated PCs during the second 24 hr of WEC (Figures 7H and 7I, arrows). Forced *Insm1* expression significantly increased this proportion (Figure 7J).

Conversely, the proportion of the mRFP and BrdU double-positive cells that were PCNA negative after 48 hr of WEC, i.e., the proportion of postmitotic cells that originated from electroporated PCs during the second 24 hr of WEC (Figures 7H and 7I, arrowheads), was significantly decreased upon forced *Insm1* expression (Figure 7K). Moreover, most of the mRFP and BrdU double-positive, PCNA-negative cells were located in the preplate, consistent with these being neurons generated from electroporated PCs during the second 24 hr of WEC. In line with this, the proportion of electroporated cells that accumulated in the preplate was significantly reduced upon forced *Insm1* expression (Figures 7H and 7I, red; data not shown).

Thus, forced *Insm1* expression reduces the targeted PCs that remain apically after the first 24 hr of WEC to about half of control (Figure 5D) but increases PCs that originate from electroporated PCs during the second 24 hr of WEC (Figure 7J). Taken together, these findings imply that the Insm1-induced doubling of basal mitoses during the second 24 hr of WEC (Figure 7A, right) reflected their generation from *Insm1*-expressing BPs. In other words, we conclude that forced *Insm1* expression in dTel NE cells at the very onset of neurogenesis, when most of these cells undergo symmetric proliferative divisions (Haubensak et al., 2004), leads to the generation of self-amplifying BPs at the expense of the generation of BPs that divide to produce neurons.

Forced Premature *Insm1* Expression Promotes Horizontal Cleavage Plane Orientation of Basal Mitoses

APs can self-renew and maintain apical-basal polarity through mitosis, and most of their cleavage planes are oriented parallel to, or deviate only slightly from, the apical-basal (radial) cell axis—i.e., they occur roughly perpendicular to the ventricular surface (vertical cleavage plane; Figure 7L, 90°–60°) (Chenn and McConnell, 1995; Götz and Huttner, 2005; Huttner and Kosodo, 2005; Konno et al., 2008; Kosodo et al., 2004; Noctor et al., 2008). By contrast, most BPs divide only once to generate two neurons, lack apical-basal polarity during mitosis, and show a nearly random cleavage plane orientation (Attardo et al., 2008; Haubensak et al., 2004; Noctor et al., 2008; Stricker et al., 2006). Given the ability of the Insm1-induced BPs to self-amplify (Figures 7A–7K), we therefore investigated whether forced *Insm1* expression affected their cleavage plane orientation.

Analysis of mitotic BPs in the dTel that were derived from PCs electroporated under control conditions at E10.5 during the ensuing 48 hr of WEC (i.e., mRFP-positive BPs) revealed a nearly random orientation of DAPI-stained chromosomes at metaphase and anaphase/telophase (Figure 7L). This was indicative of a random cleavage plane orientation and confirmed and extended previous observations (Attardo et al., 2008). In contrast, upon forced *Insm1* expression, the proportion of basal mitoses with chromosomes that were oriented parallel to the ventricular surface at metaphase and anaphase/telophase, indicative of a corresponding cleavage plane orientation (horizontal cleavage plane, 30°–0°), was increased to more than half of total (Figure 7L). These data suggest that *Insm1* expression promotes the positioning of the mitotic spindle poles of BPs along the radial axis of the cortical wall.

Downstream Effectors of Insm1

To obtain insight into Insm1 downstream target genes whose altered expression might explain the phenotypes observed upon *Insm1* ablation and forced expression, we performed comparative genome-wide gene expression profiling of the E13.5 dTel of wild-type, heterozygous, and homozygous *Insm1* knockout mouse embryos using Affymetrix microarrays. Table 1 lists the 28 genes (other than *Insm1* itself) whose expression showed a statistically significant change (adjusted p value < 0.05) between wild-type and *Insm1* knockout. Each of these genes was decreased in its mRNA expression level upon *Insm1* ablation. Of the 28 genes, 10 are known to be specifically expressed in the VZ/SVZ (Visel et al., 2004), and interestingly, at least 2 of these 10 genes, *Robo2* and *Myh9*, are involved in the balance between APs and BPs, as is discussed below.

As to potential downstream targets of Insm1 involved in cell-cycle regulation, at least six of the genes listed in Table 1 (*Elavl4*, *Nhlh1*, *Ebf3*, *Net1*, *St18*, and *Rassf2*) can be considered as candidates to mediate the cell-cycle lengthening observed upon

their expression in the E14.5 cortical wall (Visel et al., 2004): (1) "yes," specific expression in VZ and/or SVZ PCs; (2) "yes (ubiquitous)," expression in the VZ and SVZ but also in the other layers of the cortical wall; (3) "not obvious (migrating neurons)," scattered expression in VZ and/or SVZ presumably due to migrating neurons, with stronger expression in the intermediate zone and/or cortical plate; "not obvious," no detectable expression in VZ and SVZ; "ND," expression not determined in Visel et al. (2004).

[a] O. Marín, 2008, Cortical Development, speaker abstract.

forced *Insm1* expression. For gene ontology analysis and the effects of *Insm1* ablation on *Mash1* and *Hes1* mRNA, see Figures S11 and S12.

DISCUSSION

Insm1, a Panneurogenic Transcription Factor in Neural Stem and Progenitor Cells

Our study demonstrates that the transcription factor Insm1 exhibits panneurogenic expression in the developing mammalian CNS. Specifically, *Insm1* was found to be transcribed selectively in the *Tis21*-GFP-positive subpopulations of neural stem and PCs, i.e., those that divide to generate neurons or neuronally committed PCs, but not in newborn neurons. Importantly, *Insm1* is expressed in correlation with neurogenesis all along the rostrocaudal axis, in contrast to all other transcription factors studied thus far in the context of neurogenesis (e.g., the proneural genes), which show region-specific expression patterns (Duggan et al., 2008; Guillemot, 2005). Together with our observation that the various region-specific proneural genes, such as *Ngn2* (dTel) and *Mash1* (ventral telencephalon), induce *Insm1* expression (Castro et al., 2006), this suggests that Insm1 is a core constituent of a common effector pathway in neural PCs leading to neurogenesis. The upregulation of *Insm1* in APs observed in the E10.5 hindbrain of *Hes5* knockout mice, which are known to exhibit premature neurogenesis (Hatakeyama et al., 2004), is fully consistent with this notion.

Expression of *Insm1* in correlation with neurogenesis is maintained until adulthood, as evidenced by the presence of *Insm1* mRNA in the wall of the lateral ventricle, a known site of adult neurogenesis (Alvarez-Buylla and Garcia-Verdugo, 2002; Ninkovic and Götz, 2007). Moreover, the panneurogenic expression of *Insm1* is a feature conserved in evolution. As *Insm1* is specifically found in essentially all neurogenic APs and BPs in the developing mouse CNS, the *Drosophila* ortholog *nerfin-1* is expressed in virtually all delaminating neuroblasts and ganglion mother cells, the fly counterpart to neurogenic APs and BPs, respectively, but not in postmitotic neurons and glial cells (Kuzin et al., 2005).

In functional terms, analysis of the developing *Insm1* null brain reveals a panneurogenic role of Insm1 in neural PCs. Specifically, our data indicate that Insm1 contributes to neural PCs becoming committed to the neuronal lineage. This notion is consistent with the observed reduction in neurons throughout the *Insm1* null brain and the concomitant expansion of VZ PCs.

Insm1 Induces the Switch from APs to BPs

Importantly, in the dTel, this panneurogenic role of Insm1 has undergone a remarkable specification. Our loss- and gain-of-function analyses in the mouse embryo demonstrate that Insm1 is a key component of the machinery that underlies the translocation of mitoses of neural PCs from an apical to a basal position. While the forced expression of *Insm1* in the dTel neuroepithelium indicated that it is sufficient to induce basal mitoses, the reduction in BPs in the *Insm1* null dTel showed that Insm1 is required for the full extent of BPs. However, the incomplete loss of BPs in the *Insm1* null dTel suggests that this transcriptional regulator is one, but not the only, factor necessary to generate BPs. Another transcription factor reported to be involved in this process is Ngn2 (Britz et al., 2006; Miyata et al., 2004).

In considering possible underlying mechanisms, we note that the magnitude of the increase in basal mitoses observed 24 hr after transfection of *Insm1* into NE cells matched that of the decrease in apical mitoses. In light of this observation, we conclude that most of the basal mitoses induced by Insm1 within 24 hr were PCs arising from apical mitoses. Thus, together with the observations that the developing *Insm1* null neocortex shows (1) reduced cortical plate and SVZ thickness but, particularly at E16.5, (2) increased VZ thickness and (3) lateral expansion, it appears that the BP progeny in the mouse contribute primarily to cortical thickness and that the AP expansion that results from the reduced BP generation upon *Insm1* ablation leads to increased radial units and thus lateral expansion of the neocortex.

In contrast to the BPs normally observed in the dTel, 90% of which have been shown to be *Tis21*-GFP positive (Haubensak et al., 2004), most of the additional basal mitoses induced by *Insm1* expression were *Tis21*-GFP negative. This most likely reflects the fact that at E10.5, the overwhelming majority (>90%) of NE cells, which are the target of *Insm1* electroporation, are *Tis21*-GFP negative (Haubensak et al., 2004). Hence, *Insm1* expression in E10.5 NE cells is sufficient to convert these normally apically dividing PCs to basally dividing cells, but not to induce *Tis21* expression.

Almost all apically dividing NE cells (>95%) are known to be Tbr2 negative (Englund et al., 2005). Interestingly, in contrast to the lack of *Tis21*-GFP expression, essentially all of the additional basal mitoses induced by *Insm1* expression were Tbr2 positive, like the BPs normally observed in the telencephalon (Englund et al., 2005). Thus, the Insm1-induced basal mitoses show at least one other feature characteristic of BPs, i.e., Tbr2 expression. Our finding implies that Insm1 is a positive regulator of Tbr2 expression. Consistent with this conclusion, the proportion of Tbr2-positive apical mitoses was decreased in the *Insm1* knockout.

Microarray analysis revealed at least two intriguing downstream targets of Insm1, *Robo2* and *Myh9*, that might mediate its effects on APs versus BPs. Thus, recent findings (O. Marín, 2008, Cortical Development, speaker abstract) indicate that the Slit receptors Robo1 and 2 are involved not only in regulating neuronal migration (Lopez-Bendito et al., 2007) but also in modulating the balance between APs and BPs. The reduced level of *Robo2* mRNA in the E13.5 *Insm1* null dTel therefore raises the possibility that the effects of Insm1 on the level of APs versus BPs are mediated at least in part via regulation of *Robo2* levels.

As to Myh9, our group has recently found that interference with nonmuscle myosin II function by the highly specific inhibitor blebbistatin impairs the apical-to-basal delamination of PCs from the neuroepithelium, which is a key aspect of the generation of BPs (J. Schenk and W.B.H., unpublished data). Hence, the reduced level of mRNA for *Myh9*, a component of nonmuscle myosin IIA, in the E13.5 *Insm1* null dTel also provides a potential explanation for the reduction in BPs observed upon *Insm1* ablation.

Insm1 Allows the Expansion of BPs

In the *Insm1* knockout, concomitant with the partial loss of BPs, the number of neurons was substantially reduced. However,

forced expression of *Insm1* did not increase the number of neurons in parallel with that of BPs but actually decreased the accumulation of neurons. How can this seemingly paradoxical finding be explained? A key observation in this regard was that upon forced expression of *Insm1* in the E10.5 dTel neuroepithelium, basally dividing cells (rather than postmitotic neurons) accumulated over time. Given that at E10.5 the vast majority of APs (the target of *Insm1* electroporation) divide to generate more APs (symmetric proliferative divisions) (Haubensak et al., 2004; Pontious et al., 2008; Takahashi et al., 1995a), an intriguing explanation is that this PC pool-expanding mode of cell division is maintained even though, as a result of forced *Insm1* expression, mitosis now occurs in an abventricular, basal location. Direct support for this is provided by the observed increase, upon forced *Insm1* expression, in PCNA-positive PCs at 48 hr of WEC that originated from electroporated BrdU-labeled PCs during the second 24 hr of WEC. Thus, in contrast to the BPs normally observed in the rodent telencephalon, most of which divide only once to generate two postmitotic neurons (Haubensak et al., 2004; Kriegstein et al., 2006; Miyata et al., 2004; Noctor et al., 2004; Pontious et al., 2008), the additional basally dividing cells observed 24 hr after *Insm1* electroporation self-amplify, at the expense of neuron production.

Following the onset of neurogenesis in the dTel at E10.5, an increasing proportion of APs normally switch from symmetric, proliferative divisions to divisions that generate either neurons (direct neurogenic divisions) or BPs that in turn generate neurons (indirect neurogenic divisions) (Haubensak et al., 2004; Kriegstein et al., 2006; Pontious et al., 2008). A corollary of the observation that upon forced *Insm1* expression, basally dividing cells and not postmitotic neurons accumulated is that in the targeted, now basally dividing cells, this progressive switching does not take place. Hence, the consequence of *Insm1* expression, i.e., switching the site of mitosis to an abventricular, basal location, when occurring prematurely, does not suffice to induce the onset of neurogenic divisions. This conclusion is consistent with the lack of *Tis21* expression in the targeted cells.

Insm1, a Constituent of the Molecular Machinery Underlying the Evolutionary Expansion of the Mammalian Cerebral Cortex

Given that the expansion of the mammalian cerebral cortex is associated with an increase in BPs relative to APs (Bystron et al., 2008; Kriegstein et al., 2006; Pontious et al., 2008; Rakic, 2003; Smart et al., 2002; Tarabykin et al., 2001), our data imply that Insm1 is part of the molecular machinery underlying this expansion. Of particular interest in this regard is the ability of Insm1 to promote the enlargement of the pool of PCs exhibiting mitosis in a basal location without inducing their differentiation to become committed to neurogenic divisions. This capacity is what would be expected of a factor involved in the self-expansion of BPs. It will therefore be interesting to investigate whether the evolutionary increase in BP self-expansion, especially that thought to occur in primates (Fish et al., 2008; Kriegstein et al., 2006; Pontious et al., 2008), involves Insm1.

EXPERIMENTAL PROCEDURES

For detailed methods, see Supplemental Experimental Procedures.

Mice

Unless indicated otherwise, NMRI mice were used. The *Tis21*-GFP knockin line (Haubensak et al., 2004) was maintained as homozygote on the C57BL/6 background and mated with wild-type C57BL/6 females to obtain heterozygous embryos, which were used for all analyses. *Insm1* knockout embryos (C57BL/6 background) were obtained by crossing heterozygous mice (Gierl et al., 2006). On this genetic background, the *Insm1* knockout is embryonic lethal starting from E11.5; therefore, all studies were performed at E11.5–E16.5. The day of vaginal plug was defined as E0.5. Fixed *Hes1*, *Hes5*, *Ngn2*, *Mash1*, and *Ngn2/Mash1* double-knockout embryos together with wild-type as well as heterozygous littermates were generous gifts of R. Kageyama and F. Guillemot, respectively.

Microarray Analysis

dTel was dissected from mouse embryos. RNA extraction, probe synthesis, and hybridization to Affymetrix microarrays (Affymetrix, Santa Clara, CA, USA) were performed according to the manufacturer's protocol. Data processing and identification of differentially expressed genes was carried out as described previously (Gierl et al., 2006). Genes were considered differentially expressed if the difference of their expression level had a p value ≤ 0.05.

In Situ Hybridization and Immunohistology

Digoxigenin-labeled riboprobes for ISH were prepared from RT-PCR of cDNAs for *Insm1* (nt 504–1238 or nt 122–1804, AF044669) and *Tis21* (nt 12–612, NM_007570). Whole-mount ISH was performed according to standard methods. ISH and immunostaining were performed as described previously (Iacopetti et al., 1999) using 10 μm coronal cryosections unless indicated otherwise.

Whole-Embryo Culture and Electroporation

WEC of E10.5 NMRI or *Tis21*-GFP knockin mice and electroporation were performed as described previously (Osumi and Inoue, 2001; Calegari and Huttner, 2003).

ACCESSION NUMBERS

Microarray data described herein have been deposited in the NCBI Gene Expression Omnibus (http://www.ncbi.nlm.nih.gov/geo/) with the accession numbers GSM309054–GSM309071.

SUPPLEMENTAL DATA

The Supplemental Data include Supplemental Results and Discussion, Supplemental Experimental Procedures, Supplemental References, and twelve figures and can be found with this article online at http://www.neuron.org/supplemental/S0896-6273(08)00770-8.

ACKNOWLEDGMENTS

We thank Drs. J. Jaszai and V. Dubreuil for advice and helpful discussion and the facilities of MPI-CBG, especially J. Helppi and the mouse facility, for excellent support. We thank Dr. G. Thornton for helpful comments on the manuscript. W.B.H. was supported by grants from the Deutsche Forschungsgemeinschaft (DFG) (SPP 1109, Hu 275/7-3; SPP 1111, Hu 275/8-3; SFB/TR 13, B1; SFB 655, A2), by the DFG-funded Center for Regenerative Therapies Dresden, by the Fonds der Chemischen Industrie, and by the Federal Ministry of Education and Research (BMBF) in the framework of the National Genome Research Network (NGFN-2).

Accepted: September 5, 2008
Published: October 8, 2008

REFERENCES

Alvarez-Buylla, A., and Garcia-Verdugo, J.M. (2002). Neurogenesis in adult subventricular zone. J. Neurosci. *22*, 629–634.

Attardo, A., Calegari, F., Haubensak, W., Wilsch-Brauninger, M., and Huttner, W.B. (2008). Live imaging at the onset of cortical neurogenesis reveals differential appearance of the neuronal phenotype in apical versus basal progenitor progeny. PLoS ONE *3*, e2388.

Britz, O., Mattar, P., Nguyen, L., Langevin, L.M., Zimmer, C., Alam, S., Guillemot, F., and Schuurmans, C. (2006). A role for proneural genes in the maturation of cortical progenitor cells. Cereb. Cortex *16* (*Suppl 1*), i138–i151.

Buchman, J.J., and Tsai, L.H. (2007). Spindle regulation in neural precursors of flies and mammals. Nat. Rev. Neurosci. *8*, 89–100.

Bystron, I., Blakemore, C., and Rakic, P. (2008). Development of the human cerebral cortex: Boulder Committee revisited. Nat. Rev. Neurosci. *9*, 110–122.

Calegari, F., and Huttner, W.B. (2003). An inhibition of cyclin-dependent kinases that lengthens, but does not arrest, neuroepithelial cell cycle induces premature neurogenesis. J. Cell Sci. *116*, 4947–4955.

Calegari, F., Haubensak, W., Haffner, C., and Huttner, W.B. (2005). Selective lengthening of the cell cycle in the neurogenic subpopulation of neural progenitor cells during mouse brain development. J. Neurosci. *25*, 6533–6538.

Candal, E., Alunni, A., Thermes, V., Jamen, F., Joly, J.S., and Bourrat, F. (2007). Ol-insm1b, a SNAG family transcription factor involved in cell cycle arrest during medaka development. Dev. Biol. *309*, 1–17.

Cappello, S., Attardo, A., Wu, X., Iwasato, T., Itohara, S., Wilsch-Brauninger, M., Eilken, H.M., Rieger, M.A., Schroeder, T.T., Huttner, W.B., et al. (2006). The Rho-GTPase cdc42 regulates neural progenitor fate at the apical surface. Nat. Neurosci. *9*, 1099–1107.

Castro, D.S., Skowronska-Krawczyk, D., Armant, O., Donaldson, I.J., Parras, C., Hunt, C., Critchley, J.A., Nguyen, L., Gossler, A., Gottgens, B., et al. (2006). Proneural bHLH and Brn proteins coregulate a neurogenic program through cooperative binding to a conserved DNA motif. Dev. Cell *11*, 831–844.

Caviness, V.S., Jr., Takahashi, T., and Nowakowski, R.S. (1995). Numbers, time and neocortical neuronogenesis: a general developmental and evolutionary model. Trends Neurosci. *18*, 379–383.

Chenn, A., and McConnell, S.K. (1995). Cleavage orientation and the asymmetric inheritance of Notch1 immunoreactivity in mammalian neurogenesis. Cell *82*, 631–641.

Dehay, C., and Kennedy, H. (2007). Cell-cycle control and cortical development. Nat. Rev. Neurosci. *8*, 438–450.

Duggan, A., Madathany, T., de Castro, S.C., Gerrelli, D., Guddati, K., and Garcia-Anoveros, J. (2008). Transient expression of the conserved zinc finger gene INSM1 in progenitors and nascent neurons throughout embryonic and adult neurogenesis. J. Comp. Neurol. *507*, 1497–1520.

Englund, C., Fink, A., Lau, C., Pham, D., Daza, R.A., Bulfone, A., Kowalczyk, T., and Hevner, R.F. (2005). Pax6, Tbr2, and Tbr1 are expressed sequentially by radial glia, intermediate progenitor cells, and postmitotic neurons in developing neocortex. J. Neurosci. *25*, 247–251.

Fish, J.L., Dehay, C., Kennedy, H., and Huttner, W.B. (2008). Making bigger brains—the evolution of neural-progenitor-cell division. J. Cell Sci. *121*, 2783–2793.

Gal, J.S., Morozov, Y.M., Ayoub, A.E., Chatterjee, M., Rakic, P., and Haydar, T.F. (2006). Molecular and morphological heterogeneity of neural precursors in the mouse neocortical proliferative zones. J. Neurosci. *26*, 1045–1056.

Gierl, M.S., Karoulias, N., Wende, H., Strehle, M., and Birchmeier, C. (2006). The zinc-finger factor Insm1 (IA-1) is essential for the development of pancreatic beta cells and intestinal endocrine cells. Genes Dev. *20*, 2465–2478.

Goto, Y., De Silva, M.G., Toscani, A., Prabhakar, B.S., Notkins, A.L., and Lan, M.S. (1992). A novel human insulinoma-associated cDNA, IA-1, encodes a protein with "zinc-finger" DNA-binding motifs. J. Biol. Chem. *267*, 15252–15257.

Götz, M., and Huttner, W.B. (2005). The cell biology of neurogenesis. Nat. Rev. Mol. Cell Biol. *6*, 777–788.

Guillemot, F. (2005). Cellular and molecular control of neurogenesis in the mammalian telencephalon. Curr. Opin. Cell Biol. *17*, 639–647.

Hatakeyama, J., Bessho, Y., Katoh, K., Ookawara, S., Fujioka, M., Guillemot, F., and Kageyama, R. (2004). Hes genes regulate size, shape and histogenesis of the nervous system by control of the timing of neural stem cell differentiation. Development *131*, 5539–5550.

Haubensak, W., Attardo, A., Denk, W., and Huttner, W.B. (2004). Neurons arise in the basal neuroepithelium of the early mammalian telencephalon: A major site of neurogenesis. Proc. Natl. Acad. Sci. USA *101*, 3196–3201.

Huttner, W.B., and Kosodo, Y. (2005). Symmetric versus asymmetric cell division during neurogenesis in the developing vertebrate central nervous system. Curr. Opin. Cell Biol. *17*, 648–657.

Iacopetti, P., Michelini, M., Stuckmann, I., Oback, B., Aaku-Saraste, E., and Huttner, W.B. (1999). Expression of the antiproliferative gene TIS21 at the onset of neurogenesis identifies single neuroepithelial cells that switch from proliferative to neuron-generating division. Proc. Natl. Acad. Sci. USA *96*, 4639–4644.

Konno, D., Shioi, G., Shitamukai, A., Mori, A., Kiyonari, H., Miyata, T., and Matsuzaki, F. (2008). Neuroepithelial progenitors undergo LGN-dependent planar divisions to maintain self-renewability during mammalian neurogenesis. Nat. Cell Biol. *10*, 93–101.

Kosodo, Y., Röper, K., Haubensak, W., Marzesco, A.-M., Corbeil, D., and Huttner, W.B. (2004). Asymmetric distribution of the apical plasma membrane during neurogenic divisions of mammalian neuroepithelial cells. EMBO J. *23*, 2314–2324.

Kriegstein, A., Noctor, S., and Martinez-Cerdeno, V. (2006). Patterns of neural stem and progenitor cell division may underlie evolutionary cortical expansion. Nat. Rev. Neurosci. *7*, 883–890.

Kriegstein, A.R., and Götz, M. (2003). Radial glia diversity: a matter of cell fate. Glia *43*, 37–43.

Kuzin, A., Brody, T., Moore, A.W., and Odenwald, W.F. (2005). Nerfin-1 is required for early axon guidance decisions in the developing Drosophila CNS. Dev. Biol. *277*, 347–365.

Lan, M.S., Li, Q., Lu, J., Modi, W.S., and Notkins, A.L. (1994). Genomic organization, 5′-upstream sequence, and chromosomal localization of an insulinoma-associated intronless gene, IA-1. J. Biol. Chem. *269*, 14170–14174.

Lopez-Bendito, G., Flames, N., Ma, L., Fouquet, C., Di Meglio, T., Chedotal, A., Tessier-Lavigne, M., and Marin, O. (2007). Robo1 and Robo2 cooperate to control the guidance of major axonal tracts in the mammalian forebrain. J. Neurosci. *27*, 3395–3407.

Miyata, T., Kawaguchi, A., Saito, K., Kawano, M., Muto, T., and Ogawa, M. (2004). Asymmetric production of surface-dividing and non-surface-dividing cortical progenitor cells. Development *131*, 3133–3145.

Molyneaux, B.J., Arlotta, P., Menezes, J.R., and Macklis, J.D. (2007). Neuronal subtype specification in the cerebral cortex. Nat. Rev. Neurosci. *8*, 427–437.

Morin, X., Jaouen, F., and Durbec, P. (2007). Control of planar divisions by the G-protein regulator LGN maintains progenitors in the chick neuroepithelium. Nat. Neurosci. *10*, 1440–1448.

Ninkovic, J., and Götz, M. (2007). Signaling in adult neurogenesis: from stem cell niche to neuronal networks. Curr. Opin. Neurobiol. *17*, 338–344.

Noctor, S.C., Martinez-Cerdeno, V., Ivic, L., and Kriegstein, A.R. (2004). Cortical neurons arise in symmetric and asymmetric division zones and migrate through specific phases. Nat. Neurosci. *7*, 136–144.

Noctor, S.C., Martinez-Cerdeno, V., and Kriegstein, A.R. (2008). Distinct behaviors of neural stem and progenitor cells underlie cortical neurogenesis. J. Comp. Neurol. *508*, 28–44.

Osumi, N., and Inoue, T. (2001). Gene transfer into cultured mammalian embryos by electroporation. Methods *24*, 35–42.

Pontious, A., Kowalczyk, T., Englund, C., and Hevner, R.F. (2008). Role of intermediate progenitor cells in cerebral cortex development. Dev. Neurosci. *30*, 24–32.

Rakic, P. (1995). A small step for the cell, a giant leap for mankind: a hypothesis of neocortical expansion during evolution. Trends Neurosci. *18*, 383–388.

Rakic, P. (2003). Developmental and evolutionary adaptations of cortical radial glia. Cereb. Cortex *13*, 541–549.

Smart, I.H. (1972b). Proliferative characteristics of the ependymal layer during the early development of the mouse diencephalon, as revealed by recording the number, location, and plane of cleavage of mitotic figures. J. Anat. *113*, 109–129.

Smart, I.H., Dehay, C., Giroud, P., Berland, M., and Kennedy, H. (2002). Unique morphological features of the proliferative zones and postmitotic compartments of the neural epithelium giving rise to striate and extrastriate cortex in the monkey. Cereb. Cortex *12*, 37–53.

Stricker, S.H., Meiri, K., and Götz, M. (2006). P-GAP-43 is enriched in horizontal cell divisions throughout rat cortical development. Cereb. Cortex *16* (*Suppl 1*), i121–i131.

Takahashi, T., Nowakowski, R.S., and Caviness, V.S., Jr. (1995a). Early ontogeny of the secondary proliferative population of the embryonic murine cerebral wall. J. Neurosci. *15*, 6058–6068.

Takahashi, T., Nowakowski, R.S., and Caviness, V.S., Jr. (1995b). The cell cycle of the pseudostratified ventricular epithelium of the embryonic murine cerebral wall. J. Neurosci. *15*, 6046–6057.

Tarabykin, V., Stoykova, A., Usman, N., and Gruss, P. (2001). Cortical upper layer neurons derive from the subventricular zone as indicated by Svet1 gene expression. Development *128*, 1983–1993.

Visel, A., Thaller, C., and Eichele, G. (2004). GenePaint.org: an atlas of gene expression patterns in the mouse embryo. Nucleic Acids Res. *32*, D552–D556.

Wildner, H., Gierl, M.S., Strehle, M., Pla, P., and Birchmeier, C. (2007). Insm1 (IA-1) is a crucial component of the transcriptional network that controls differentiation of the sympatho-adrenal lineage. Development *135*, 473–481.

Xie, J., Cai, T., Zhang, H., Lan, M.S., and Notkins, A.L. (2002). The zinc-finger transcription factor INSM1 is expressed during embryo development and interacts with the Cbl-associated protein. Genomics *80*, 54–61.